OPEN

Ordering Ag nanowire arrays by a glass capillary: A portable, reusable and durable SERS substrate

Jian-Wei Liu[1], Jin-Long Wang[1], Wei-Ran Huang[1], Le Yu[2], Xi-Feng Ren[2], Wu-Cheng Wen[1] & Shu-Hong Yu[1]

[1]Division of Nanomaterials & Chemistry, Hefei National Laboratory for Physical Sciences at Microscale, Department of Chemistry, CAS Key Laboratory of Mechanical Behavior and Design of Materials, the National Synchrotron Radiation Laboratory, University of Science and Technology of China, Hefei 230026, P. R. China, [2]Key Laboratory of Quantum Information, University of Science and Technology of China, Hefei 230026, P. R. China.

Assembly of nanowires into ordered macroscopic structures with new functionalities has been a recent focus. In this Letter, we report a new route for ordering hydrophilic Ag nanowires with high aspect ratio by flowing through a glass capillary. The present glass capillary with well-defined silver nanowire films inside can serve as a portable and reusable substrate for surface-enhanced Raman spectroscopy (SERS), which may provide a versatile and promising platform for detecting mixture pollutions. By controlling the flow parameters of nanowire suspensions, initially random Ag nanowires can be aligned to form nanowire arrays with tunable density, forming cambered nanowire films adhered onto the inner wall of the capillary. Compared with the planar ordered Ag nanowire films by the Langmuir-Blodgett (LB) technique, the cambered nanowire films show better SERS performance.

Within the past few decades, synthesis and characterization of one-dimensional (1-D) nanostructures have been made tremendous advances owing to their unique structures and potential applications[1–3]. With significant advancement in 1-D nanomaterials, a wide range of assembly strategies have been developed to create and construct functional well-defined ordered superstructures or complex architectures with desired properties[4–7]. A variety of principles and strategies have been used to assemble nanowires, such as (i) external fields based assembly, in which external field would affect the directional aggregation of nanowire blocks, resulting in the formation of well-aligned structures of magnetic or charged nanowires[8,9], (ii) interface based assembly, in which interfaces offer a significant platform for the organization of nanowire blocks based on interfacial-ordering effects, especially for evaporation induce assembly and Langmuir-Blodgett (LB) technique[10–18], and (iii) other assembly methods, such as fluid flow[19–21], pattern transfer process[22], blown bubble[23], electrospinning[24–26], and mechanical force[27–30]. Compared with the sophisticated manufacturing of macroscopic devices, the assembly and integration of nanoscale objects into nanodevices are far from perfect and major efforts are still needed to further develop nanowire assembly strategies to expand expected potentials[31–33].

In the past decades, research on surface-enhanced Raman spectroscopy (SERS) has inspired an intense effort in the fields of physics, chemistry, biology, and biomedicine to explore its potential applications[34,35]. Various metallic nanostructured SERS substrates have been fabricated due to the introduction of Raman hot spots[36]. Although disordered Ag nanowires assembled into ordered Ag nanowire films have been reported previously to test their SERS[13,37–39], it is of great importance to develop simple, and low-cost assembly methods to fabricate portable and reusable Ag nanowire SERS substrates.

Herein, we describe a new route for ordering hydrophilic Ag nanowires with high aspect ratio by flowing through a capillary. The formation process is strongly dependent on the flow parameters, such as flow rate and flow distance. The polarization and structural ordering were confirmed by the fluorescence enhancement which was correlated with the angle between excitation light polarization and the silver nanowire direction. The glass capillary with well-defined Ag nanowire films inside can serve as a portable, reusable and durable surface-enhanced Raman scattering (SERS) substrate with high sensitivity, using Rhodamine 6G (R6G), and 4-mercaptobenzoic acid (4-MBA) as probing molecules.

Results

Ag nanowires aligned inside of a glass capillary. Firstly, uniform and hydrophilic Ag nanowires with a diameter of 80–100 nm and aspect ratio of at least 200 were systhesized by a modified method described previously[40]. The
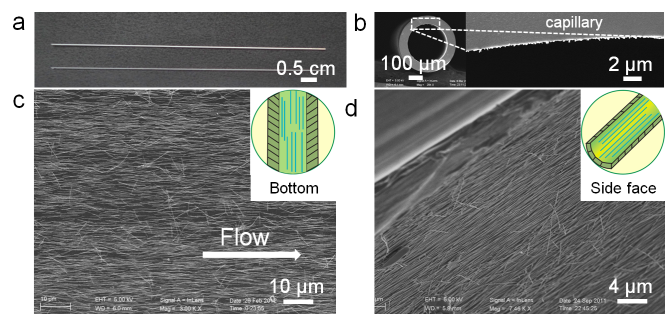
Figure 1 | Well-aligned Ag nanowire films with curvature were obtained by an ordinary glass capillary. (a) Photograph of two capillaries, upper one with the aligned Ag nanowires inside and down one is the naked capillary. (b) SEM images of the cross section of a typical capillary with Ag nanowire films inside. (c, d) SEM images of as obtained Ag nanowire assemblies at the bottom and side face of the capillary in wall. The arrow in (c) indicates the flow direction. Insets of (c, d) illustrate the position of the capillary. The experiments were carried out with a 0.154 mol/L of Ag nanowire ethanol suspensions flowing through a 300 μm capillary with a flow rate of 800 μL min^{-1}.

obtained products were confirmed by analysis of X-ray diffraction, scanning electron microscope (SEM) image, and transmission electron microscope (TEM) image (see Supplementary Information, Figs. S1, S2). The Ag nanowires were then assembled using the novel capillary induced approach.

Briefly, a 0.154 mol/L of Ag nanowire ethanol suspension was passed through a common capillary at a flow rate of 800 μL min^{-1} and well-defined parallel arrays of NWs can be successfully achieved. Fig. 1a presents the optical photograph of two capillaries, upper one with the aligned Ag nanowire films inside and down one is a naked capillary. Compared with the naked capillary, the capillary with the Ag nanowire films inside was very smooth and sparkling, indicating that the Ag nanowires were successfully well aligned in this process. The diameter of a common glass capillary we used here is around 300 μm as confirmed by SEM image (Fig. 1b). The cross section of the glass capillary with Ag nanowires aligned inside was shown by a higher magnification SEM image. The inner wall of a capillary covered with well-aligned Ag nanowires was depicted in Fig. 1c with a higher magnification, showing that most of the NWs are aligned along one direction, *i.e.*, the flowing direction. Meanwhile, there are also some small deviations with respect to the flow direction. Besides the bottom of the capillary, the side face of the capillary is also covered by aligned side-by-side Ag NWs (Fig. 1d).

A series of experiments have been carried out to understand the factors controlling the alignment of the Ag nanowires. The formation process is strongly dependent on the conditions such as the wettability, flow rate, flow distance, and the concentration of Ag nanowire suspension. To investigate the wettability responsible for this controlled assembly, it was found that there were no Ag nanowire films on the inner wall when the superhydrophobic Teflon capillary was used. When the Ag nanowire suspensions flows through a capillary, disordered nanowires becomes ordered gradually. Fig. 2a shows the photograph of an Ag nanowire covered capillary. The arrow indicates the flow direction. When the flow distance is more than about 2 cm, most of the nanowires are well aligned (Fig. 2b–e). Just as reported previously[19], the flow rate plays an important role in microfluidic flow process. That is, with increasing flow rates, from 200 to 400 and 800 μL min^{-1}, the degree of nanowire ordering was increasing (Fig. 2f–i). While, when the flow rate increases up to 1000 μL min^{-1}, the density and the degree of nanowire ordering decrease. Higher flow rate produces larger shear force and hence leads to better alignment, however, too high flow rate results in decreasing the force between the capillary and the nanowires. Moreover, the influence of the concentrations of the nanowire suspensions on the assembly of Ag nanowires was investigated. It was found that the concentration plays an important role in the density of the nanowire films (Fig. 2j–m).

Using this facile approach, Ag nanowires were closely packed and aligned parallel to each other sticking onto the capillary wall and forming a confined and uneven nanowire film. The driving force of the self-assembly process might be the van der Waals and interactions that occur between the side chains of polyvinylpyrrolidone (PVP) coated Ag nanowires and the sidewalls of capillary. These
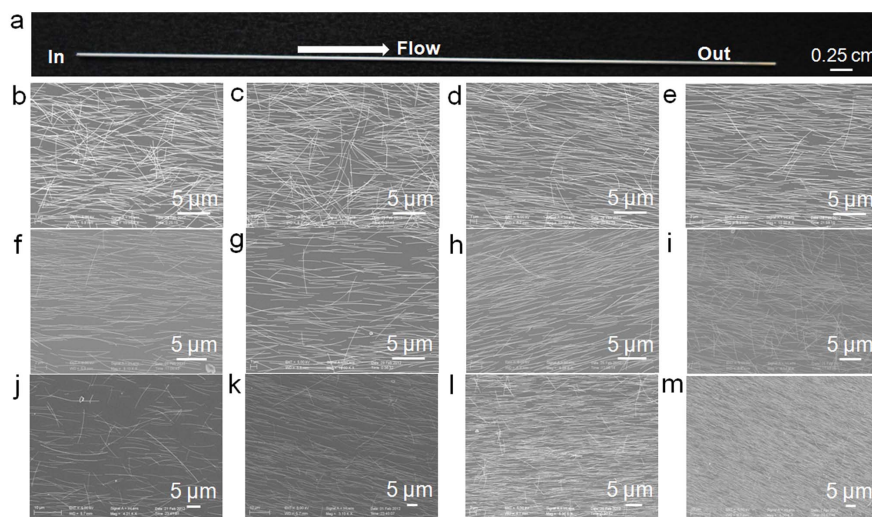
Figure 2 | Influence of the flowing factors on the assembly of Ag nanowires. (a) Photograph of an Ag nanowire covered capillary. The arrow indicates the flow directions. (b–e) Influence of the flow distance on the assembly of Ag nanowires shown by SEM images, from b to e, the flow distances are, 0, 1, 2, 3 cm, respectively. The samples prepared by 0.154 mol/L of Ag nanowire ethanol suspension flow through a 300 μm capillary with the flow rate of 800 μL min^{-1}. (f–i) Influence of the flow rate on the assembly of Ag nanowires shown by SEM images, from f to i, the flow rates are, 100, 400, 800, 1000 μL min^{-1}, respectively. The samples prepared by 0.154 mol/L of Ag nanowire ethanol suspension flow through a 300 μm capillary with different flow rate. (j–m) Influence of the concentration of the nanowire suspension on the assembly of Ag nanowires shown by SEM images, from j–m, the concentrations are, 0.031, 0.039, 0.077, 0.154 mol/L, respectively. The samples prepared by different concentrations of Ag nanowire ethanol suspension flow through a 300 μm capillary with the flow rate of 800 μL min^{-1}.

surface forces allow the assembly of one-dimensional Ag nanowires adsorbed and assembly along the axis of a capillary, without any extra pretreatment or functionalization. Interestingly, this general approach can be extended to organize other nanowires, such as ultrathin Te nanowires with different aspect ratios (see Supplementary Information, Fig. S3). Uniform Te nanowires with different aspect ratios were synthesized by modified methods described previously[41,42]. The glass capillary substrate functionalized by immersing in a 1 mM chloroform solution of 3-aminopropyltriethoxysilane (APTES) for 30 min, followed by heating at 110°C for 10 min, indicating that there is no obvious improvement in ordering formation process (see Supplementary Information, Fig. S4). Thus, common commercial glass capillary used here is more economical[19].

Optical properties of the novel well-defined Ag nanowire films inside of the capillary. The novel polarized optical transmission through periodic nanostructures has attracted much attention due to the exciting applications[43,44]. The polarization of the incident light determines the mode of excited surface plasmon which is related to the periodic structure. The setup of the experiment is illustrated in Fig. 3a. The plot shows the transmission efficiencies of different wavelength light for our sample. In our experiments, the transmission efficiency is strongly dependent on the angle of ordered nanowires and the incident light polarization. We attributed this phenomenon to the effect of the surface plasmons. Transmission spectra of the capillary with well-defined Ag nanowire films inside were recorded

by a spectrograph through a fiber (Fig. 3b). Briefly, white light from a stabilized tungsten-halogen source passed through a single mode fiber and a polarizer (only vertically polarized light can pass), then illuminated the sample. The polarization angle θ is defined as between the incident light, and the long axis of the capillary. The sample was set between two lenses of 35 mm focal length, so that the light was normally incident on the sample. The light exiting from the sample was launched into the spectrograph. The sample was rotated anti-clockwise in the plane perpendicular to the illuminating light, with the rotation angle from 0° to 360°. Transmission spectra of the sample with rotation angle $\theta = 0°$ and 90° were given in Fig. 3b. From $\theta = 0°$ to 360°, 18 curves were recorded and the intensity of Fig. 3c show the integral of the spectra peak at about 650 nm. It was found that the intensity of the transmittance as a function of rotation angles θ, and data in Fig. 3d was transferred in polar coordinates. Based on the experimental data, we presume that only light with the vertical to the nanowire alignment can stimulate the surface plasmon polaritons (SPPs), making the vertical component of the electric field worked, that is $E\sin\theta$. While, according to the energy, it should be $E^2\sin^2\theta$. Considering the background and the factor, the function relation should be:

$$S = a\left(\sin^2\theta + b\right)$$

Using the least square method, we can get the value of $a = 460706$, and $b = 1.50$. The goodness-of-fit values, $R^2 = 0.99997$, plotted against S (see Supplementary Information, Fig. S5).
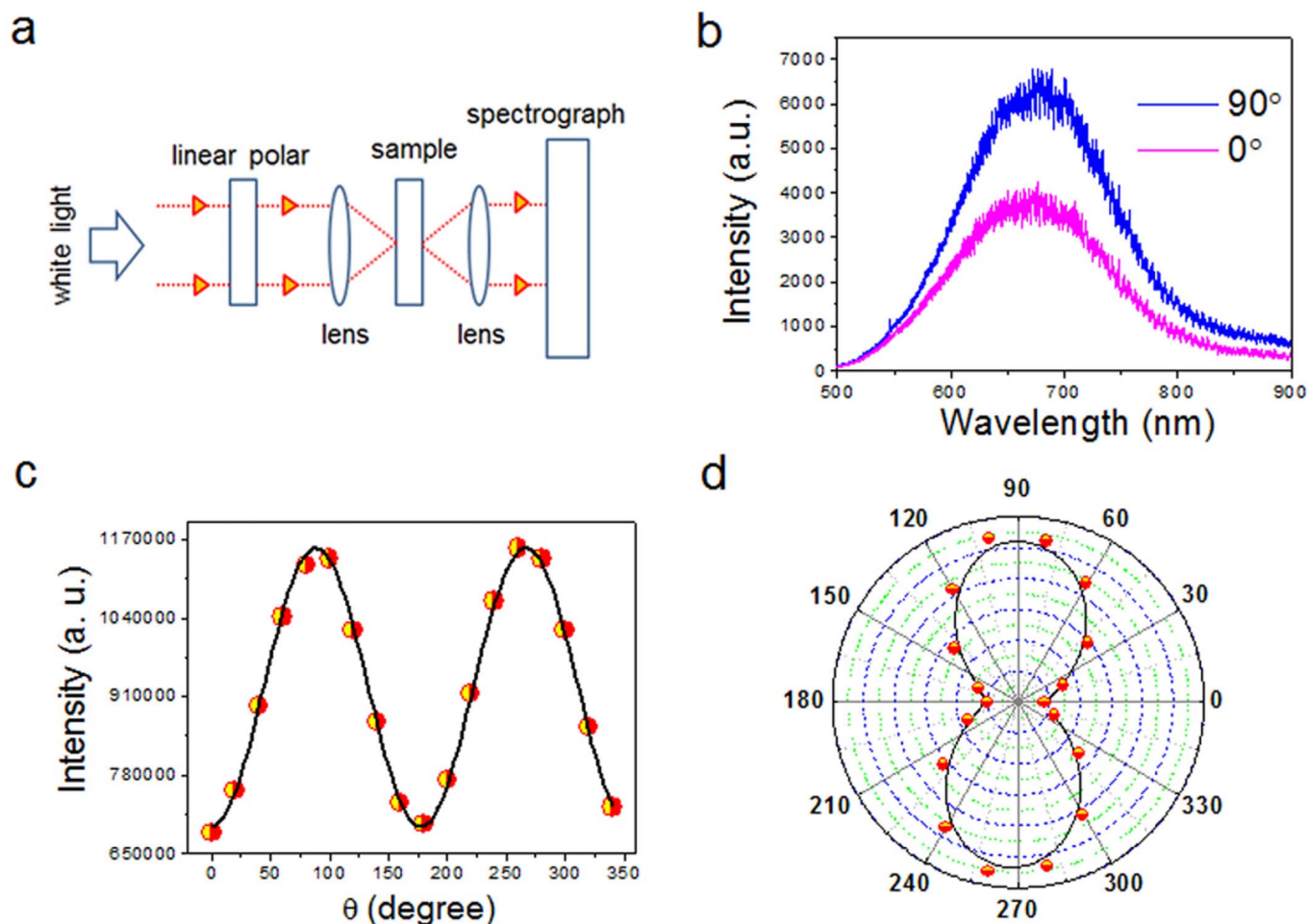
Figure 3 | Optical transmission spectra through periodic Ag nanowire films. (a) Schematic illustration of the experimental setup. polarization angle θ is defined as the angle between the polarization direction and the long nanowire axis. (b) Transmission spectra of the film of silver nanowires. The rotation angles are 0° and 90°, respectively. (c) Intensity of the transmittance as a function of rotation angles θ. (d) The data in (c) was transferred in polar coordinates. Dots: experimental data; line: fitting curve.
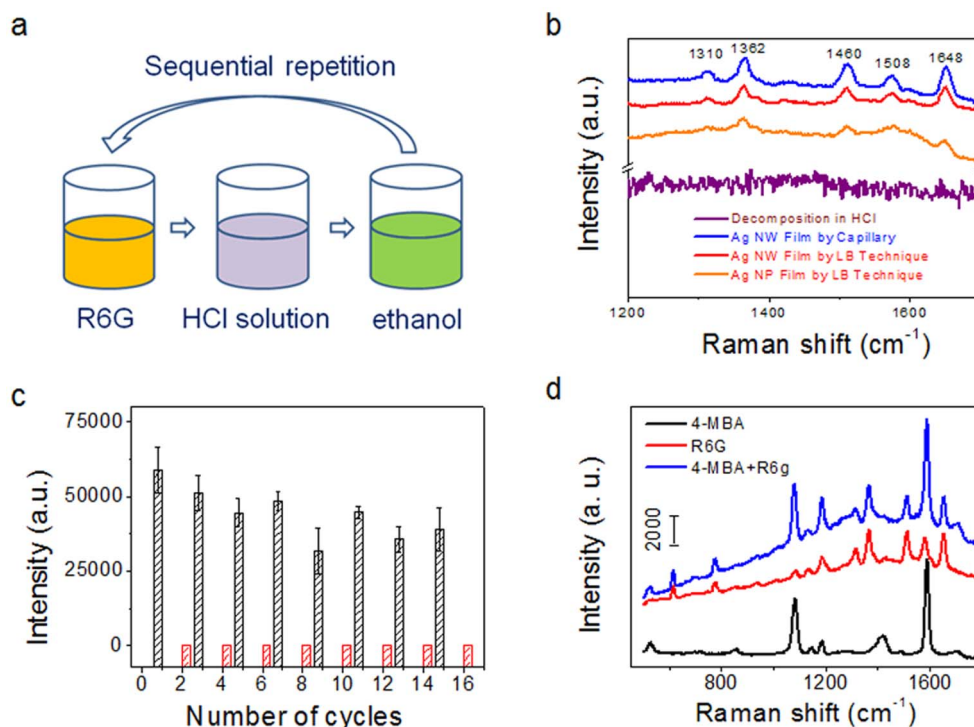
Figure 4 | Unique SERS applications of cambered Ag nanowire films inside of a glass capillary. (a) Schematic of the cyclic utilization of SERS substrate. (b) SERS spectra of adsorbed Rhodamine 6G (1×10^{-7} mol/L) before (blue) and after (purple) the dispersion into the concentrated hydrochloric acid (37.5%, wt %), SERS spectra (red) of Ag nanowire films by LB technique, and SERS spectrum (orange) of Ag colloid nanoparticle films by LB technique. (c) Repeatability of the reusable capillary SERS substrate about 8 cycles. The SERS intensities of the peak at 1362 cm^{-1} before (black) and after (red) dispersion into the concentrated hydrochloric acid as a function of number of cycles. (d) SERS spectra of adsorbed R6G, 4-MBA, and a mixture of R6G and 4-MBA.

SERS applications of cambered Ag nanowire films inside of a glass capillary. Because of the existence of the large electromagnetic (EM) field, the integrated silver nanowire films based capillary assembly can act as an active platform for portable and reusable SERS detection[13,37]. The enhanced electric field around the noble metal nanostructures is considered to be the dominant factor for the corresponding SERS enhancement. Various Ag nanostructures have been investigated as highly sensitive substrates, such as, nanoparticles (NPs)[45], nanowires (NWs)[46–48], vertically-aligned nanorods (NRs)[49,50], nanoplates[51], and so on[52]. Fig. 4a shows the schematic illustration of the cyclic utilization of SERS substrate. The vibration signatures are characteristic of Rhodamine 6G (R6G) molecules, which agree well with the Raman shifts reported in the previous literature[13] and exhibit five most prominent Raman peaks at 1310, 1362, 1460, 1508, and 1648 cm^{-1}, respectively (labeled in Fig. 4b). Eight cycles can be performed to test the stability of the Raman performance (see Supplementary Information, Fig. S6). The ordered Ag nanowires were well arranged in a confined capillary forming a unique structure which will open up potential applications. For example, compared with Ag nanowire films in planar Raman substrates by the LB technique, the Raman enhancement in our experiments is bigger, which is shown by red line in Fig. 4b (see Supplementary Information, Fig. S7)[13,37]. While, SERS spectrum of Fig. 4b (orange line) shows that Ag colloid nanoparticle films exhibit the worst performance.

Discussion

Compared with ordered Ag nanowire films by capillary, even by LB technique, the SERS performance of disordered Ag nanowire SERS substrates shows unstable (Fig. 5a and Fig. 5b). In order to make it clear, we fabricate some glass capillaries with different bending radius using oxyhydrogen flame by ourselves. With the bending radius of the glass capillary increasing, the SERS performance turns better (Fig. 5c). The detection limit of the SERS spectra for adsorbed Rhodamine 6G on Ag nanowire substrates is as low as 5×10^{-9} M (see Supplementary Information, Fig. S8). The Ag nanowire films aligned inside of the capillary will benefit to make the SERS substrates portable and reusable. After the SERS substrates using R6G as the probe molecule immersed in the concentrated hydrochloric acid liquid, no Raman signal will be detected (purple line in Fig. 4b). Based on this phenomenon, the Ag nanowire films in capillary can be used as a portable, reusable and durable substrate. Fig. 4c shows that the SERS substrate gives fairly reproducible results of the reusable phenomena after 8 numbers of cycles. Error bars were added to test the stability. The intensity of Fig. 4c is the integral area of peak of the spectra at about 1362 cm^{-1}. The concentration of R6G was used for the reusability test is 10^{-7} mol/L. The results show no state disturbance, that is no overlap of a high SERS state (black) and a low Raman signals (red). Furthermore, one of the most important applications of the SERS substrate is for the detection of pollutants, however, the samples are always mixture pollutions in practical applications. Thus, a dynamic detection of a mixture is important. To exploit the applications of the unique structured Ag nanowire films, Fig. 4d shows the SERS spectra of probing molecules, 4-MBA, R6G and the mixture of 4-MBA and R6G, respectively. Compared with the three spectra, the capillary based SERS substrate shows to be a versatile platform that can even detect mixture pollutions. The ordering of the nanowire alignment can be largely influenced by the flow rate in microfluidic flow process. In our opinion, the difference in the degree of nanowire ordering results in different SERS performance. SEM images in Figs. 2f–2i indicated that the degree of nanowire ordering was increasing with increasing flow rates from 200 to 400 and 800 μL min^{-1}. However, when the flow rate increases up to 1000 μL min^{-1}, the density and degree of the alignment of the
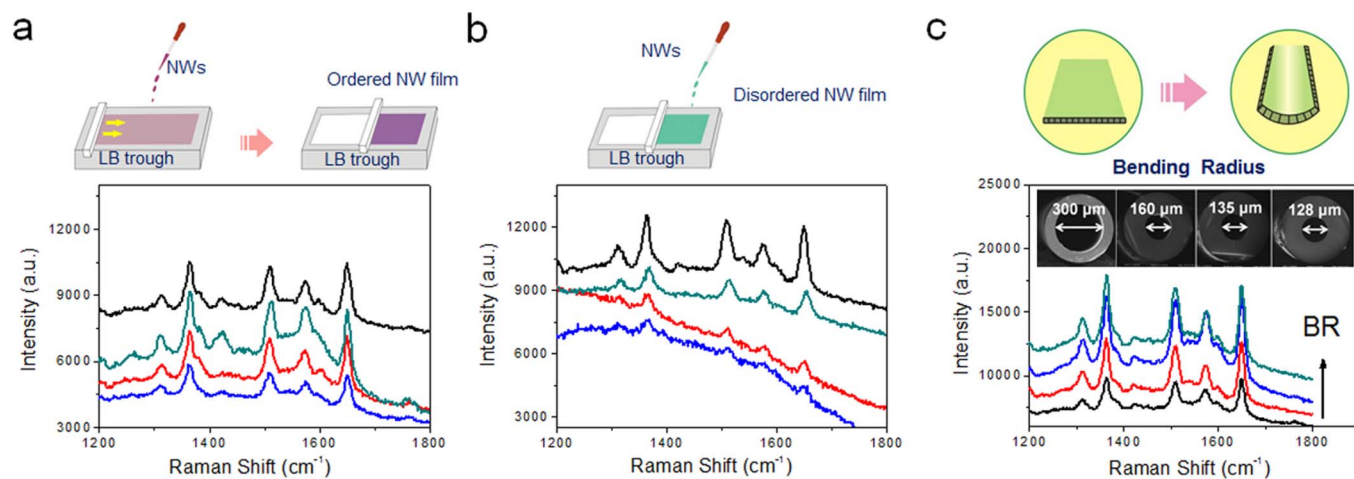
Figure 5 | SERS performances of ordered, disordered and cambered Ag nanowire films. SERS performances of (a) ordered Ag nanowire films, (b) disordered Ag nanowire films at water-air interface by LB trough with the same Ag nanowire number per unit area, and (c) ordered Ag nanowire films in glass capillaries with different bending radius. The samples prepared by adding 1 mg of the freshly prepared AgNWs into the mixed solution (0.5 mL of *N, N*-dimethylformamide (DMF) and 0.5 mL of $CHCl_3$) to form a homogeneous solution at room temperature, a 50 μL syringe was used to dispense Ag nanowire suspension onto the water subphase of the LB trough drop by drop. (Adsorbed Rhodamine 6G on Ag nanowire substrates, 514 nm excitation; power, 1 mW; data collection, 10 s).

nanowires decrease. The SERS spectra of the Ag nanowire films in the glass capillaries fabricated under different flow rates indicate that the SERS performance is largely dependent on the density and the degree of nanowire ordering (Supplementary Information, Fig. S9).

In summary, we report a new route for ordering hydrophilic Ag nanowires with high aspect ratios by flowing through a glass capillary. The formation process of ordered nanowire films on the wall of a glass capillary is strongly dependent on the flow parameters, such as flow rate, flow distance and the concentration of Ag nanowire suspensions. The structure ordering could be indirectly demonstrated by polarized transmission spectra, which represents best fits using a $sin^2\theta$ function. The cambered nanowire films facilely fabricated by this capillary induced strategy display unique ordered structure and have some advantages including against being polluted or destroyed. The present glass capillary with well-defined silver nanowire films inside can serve as a portable, reusable and durable SERS substrate, which may provide a versatile and promising platform for detecting the pollutions in environment.

Methods

All chemicals are of analytical grade and were used as received without further purification.

Synthesis of Ag nanowires. All chemicals and solvents were purchased from Shanghai Chemical Reagent Co. Ltd. and used without further purification. Uniform Ag nanowires with high aspect ratios were prepared by the polyol process method[40]. Briefly, 1.76 g of polyvinylpyrrolidone (PVP, $M_W \approx 40,000$) was added into 57 mL of glycerol in a round bottle flask and kept the solution at 85°C for one hour to form a homogeneous solution. After cool to room temperature naturally, 0.474 g of $AgNO_3$ was added into the solution. Then a NaCl solution (17.7 mg of NaCl dissolving in 0.15 mL of deionized water and 3 mL of glycerol) was added into the flask. The flask was heated from room temperature to 210°C in 20 minutes with stirring. When the temperature reached 210°C, the heating was stopped. Then 60 mL of deionized water was added and the temperature dropped to room temperature. The color of the solution turned from pale white into light brown, red, dark gray, and eventually gray-green. Keep the solution undisturbed for 48 hours to remove the Ag nanoparticles. And the obtained Ag nanowires were washed with water for three times by centrifugation at 4000 rpm for 1 min. Finally, the products were dissolved in 20 mL of ethanol.

Synthesis of Te nanowires with different aspect ratios. The synthesis of uniform Te nanowires was described previously[41,42]. The Te nanowires with the diameter of 7 nm and aspect ratio of 1000 were produced as flows: 1.0000 g of Poly(vinyl pyrrolidone) (PVP, Shanghai Reagent Company, $M_W \approx 40,000$), 0.0922 g of Na_2TeO_3, and 33 mL of double distilled water were mixed in a 50 mL Teflon-lined stainless steel autoclave. The mixture was stirred by magnetic stirring to form a homogeneous solution. Then, 1.67 mL of hydrazine hydrate (85%, wt %) and 3.33 mL of aqueous ammonia

solution (25–28%, wt %) were added into the mixed solution, respectively. After vigorous magnetic stirring for 5 min., the container was closed and maintained at 180°C for 3 h. After that, the autoclave was cooled to room temperature naturally. Te nanowires with low aspect ratio can be obtained in a typical synthesis. 20 mmol NaOH and 0.6 g poly(vinyl pyrrolidone) (PVP, Shanghai Reagent Company, $M_W \approx 40,000$) were mixed together in 50 ml EG. 3 mmol TeO_2 was then dissolved in the above stock solution at about 120°C. After the addition of 0.3 mL $N_2H_4 \cdot H_2O$ at 160°C, the Te nanowires can be obtained after reaction for about 20 min.

Assembly of Ag nanowires. A 10 mL syringe was first connected with the capillary using polytetrafluoroethylene (PTFE) capillary as bridge. 0.154 mmol Ag nanowires were added into 10 mL of ethanol stirring for 5 minutes to form a homogeneous solution at room temperature. Then, the Ag nanowire suspension was put into the prepared syringe and injected at the flow rate of 800 μL min⁻¹. Finally, 1 mL pure ethanol was introduced to flow through the capillary with the same flow rate. The sample was dried at 37°C for 4 hours.

Assembly of Ag nanowires by the LB technique. The ordered Ag nanowires monolayer was prepared using a modified Langmuir-Blodgett technique described previously[12,53]. Millipore Milli-Q water (resistivity 18.2 MΩ cm) was used as a subphase filled in the LB trough (Nima Technology, 312D). 1 mg of the freshly prepared AgNWs was dispersed into the mixed solution (0.5 mL of *N, N*-dimethylformamide (DMF) and 0.5 mL of $CHCl_3$) to form a homogeneous solution at room temperature. After that, a 50 μL syringe was used to dispense Ag nanowire suspension onto the water subphase drop by drop. Thirty minutes later, the nanowires surface layer was then compressed with a compression rate of 20 cm² min⁻¹. The constant surface pressure was kept constant as soon as the fold formation that paralleled to the barrier direction occurred.

Preparation of SERS samples. The capillary with well-aligned Ag nanowire films inside and the Ag nanowire film substrate by the LB technique were dipped into the 10^{-7} M R6G solution (10^{-4} M 4-MBA) for saturation adsorption, then taken into the oven of 60°C for the evaporate of the ethanol. For the mixture of 4-MBA and R6G, 1 mL 10^{-6} M R6G and 1 mL 10^{-3} M 4-MBA solutions were firstly mixed, then repeating the above steps.

Instruments. The X-ray diffraction patterns (XRD) were measured on a Philips X'Pert Pro Super X-ray diffractometer equipped with graphite-monochromatized Cu KR radiation. Field-emission scanning electron microscopy (FESEM) was carried out with a field emission scanning electron microanalyzer (Zeiss Supra 40 scanning electron microscope at an acceleration voltage of 5 kV. Raman scattering spectra were recorded with a JY LabRam HR 800 spectrometer using the 514 nm line of Ar+ for excitation. UV-vis spectra were recorded on UV-2501PC/2550 at room temperature (Shimadzu Corporation, Japan).Transmission electron microscopes (TEM) carried out on a commercial JEOL-7650 transmission electron microscope operated at an accelerating voltage of 100 kV.

1. Xia, Y. N., Yang, P. D., Sun, Y. G., Wu, Y. Y., Mayers, B., Gates, B., Yin, Y. D., Kim, F. & Yan, Y. Q. One-dimensional nanostructures: Synthesis, characterization, and applications. *Adv. Mater.* **15**, 353–389 (2003).

2. Hochbaum, A. I. & Yang, P. D. Semiconductor Nanowires for Energy Conversion. *Chem. Rev.* **110**, 527–546 (2010).

3. Qin, Y., Wang, X. D. & Wang, Z. L. Microfibre-nanowire hybrid structure for energy scavenging. *Nature* **451**, 809–U805 (2008).

4. Liu, J. W., Liang, H. W. & Yu, S. H. Macroscopic Scale Assembled Nanowire Thin Films and Their Functionalities. *Chem. Rev.* **112**, 4770–4799 (2012).

5. Sánchez-Iglesias, A., Grzelczak, M., Pérez-Juste, J. & Liz-Marzán, L. M. Binary Self-Assembly of Gold Nanowires with Nanospheres and Nanorods. *Angew. Chem. Int. Ed.* **49**, 9985–9989 (2010).

6. Yan, H., Choe et al. Programmable nanowire circuits for nanoprocessors. *Nature* **470**, 240–244 (2011).

7. Rogers, J. A., Ahn, J. H., Kim, H. S., Lee, K. J., Jeon, S., Kang, S. J., Sun, Y. G. & Nuzzo, R. G. Heterogeneous three-dimensional electronics by use of printed semiconductor nanomaterials. *Science* **314**, 1754–1757 (2006).

8. Freer, E. M., Grachev, O., Duan, X. F., Martin, S. & Stumbo, D. P. High-yield self-limiting single-nanowire assembly with dielectrophoresis. *Nat. Nanotechnol.* **5**, 525–530 (2010).

9. Wang, B., Ma, Y. F., Li, N., Wu, Y. P., Li, F. F. & Chen, Y. S. Facile and Scalable Fabrication of Well-Aligned and Closely Packed Single-Walled Carbon Nanotube Films on Various Substrates. *Adv. Mater.* **22**, 3067–3070 (2010).

10. Wang, Z. et al. One-Step Self-Assembly, Alignment, and Patterning of Organic Semiconductor Nanowires by Controlled Evaporation of Confined Microfluids. *Angew. Chem.Int. Ed.* **50**, 2811–2815 (2011).

11. Kim, F., Kwan, S., Akana, J. & Yang, P. D. Langmuir-Blodgett nanorod assembly. *J. Am. Chem. Soc.* **123**, 4360–4361 (2001).

12. Liu, J. W., Zhu, J. H., Zhang, C. L., Liang, H. W. & Yu, S. H. Mesostructured Assemblies of Ultrathin Superlong Tellurium Nanowires and Their Photoconductivity. *J. Am. Chem. Soc.* **132**, 8945–8952 (2010).

13. Shi, H. Y. et al. Ordering of Disordered Nanowires: Spontaneous Formation of Highly Aligned, Ultralong Ag Nanowire Films at Oil-Water-Air Interface. *Adv. Funct. Mater.* **20**, 958–964 (2010).

14. Duan, H. W., Wang, D. Y., Kurth, D. G. & Mohwald, H. Directing self-assembly of nanoparticles at water/oil interfaces. *Angew. Chem. Int. Ed.* **43**, 5639–5642 (2004).

15. Reincke, F., Hickey, S. G., Kegel, W. K. & Vanmaekelbergh, D. Spontaneous assembly of a monolayer of charged gold nanocrystals at the water/oil interface. *Angew. Chem. Int. Ed.* **43**, 458–462 (2004).

16. Liu, J. W., Zhang, S. Y., Qi, H., Wen, W. C. & Yu, S. H. A General Strategy for Macroscopic Scale Self-Assembly of Nano-Building Blocks on Liquid-Liquid Interface. *Small*, **8**, 2412–2420 (2012).

17. Whang, D., Jin, S. & Lieber, C. M. Nanolithography using hierarchically assembled nanowire masks. *Nano Lett.* **3**, 951–954 (2003).

18. Whang, D., Jin, S., Wu, Y. & Lieber, C. M. Large-scale hierarchical organization of nanowire arrays for integrated nanosystems. *Nano Lett.* **3**, 1255–1259 (2003).

19. Huang, Y., Duan, X. F., Wei, Q. Q. & Lieber, C. M. Directed assembly of one-dimensional nanostructures into functional networks. *Science* **291**, 630–633 (2001).

20. Li, Y., Yuan, B., Ji, H., Han, D., Chen, S., Tian, F. & Jiang, X. A Method for Patterning Multiple Types of Cells by Using Electrochemical Desorption of Self-Assembled Monolayers within Microfluidic Channels. *Angew. Chem. Int. Ed.* **46**, 1094–1096 (2007).

21. Park, J. S., Han, T. H., Oh, J. K. & Kim, S. O. Capillarity Induced Large Area Patterning of Peptide Nanowires. *J. Nanosci. Nanotechnol.* **10**, 6954–6957 (2010).

22. Liu, J. W., Xu, J., Liang, H. W., Wang, K. & Yu, S. H. Macroscopic Ordered Ultrathin Telluride Hetero-Nanowire Films. *Angew. Chem. Int. Ed.* **51**, 7420–7425 (2012).

23. Yu, G. H., Cao, A. Y. & Lieber, C. M. Large-area blown bubble films of aligned nanowires and carbon nanotubes. *Nat. Nanotechnol.* **2**, 372–377 (2007).

24. Yang, H., Liu, Y. Q., Zhang, X. P. & Xia, Y. N. Magnetic-Field-Assisted Electrospinning of Aligned Straight and Wavy Polymeric Nanofibers. *Adv. Mater.* **22**, 2454–2457 (2010).

25. Yang, D. Y., Lu, B., Zhao, Y. & Jiang, X. Y. Fabrication of aligned fibirous arrays by magnetic electrospinning. *Adv. Mater.* **19**, 3702–3706 (2007).

26. Li, D. & Xia, Y. N. Electrospinning of nanofibers: Reinventing the wheel? *Adv. Mater.* **16**, 1151–1170 (2004).

27. Fan, Z. Y. et al. Wafer-scale assembly of highly ordered semiconductor nanowire arrays by contact printing. *Nano Lett.* **8**, 20–25 (2008).

28. Pevzner, A. et al. Knocking Down Highly-Ordered Large-Scale Nanowire Arrays. *Nano Lett.* **10**, 1202 (2010).

29. Cui, X. J., Li, L. M., Xu, J. & Xu, F. Fabrication of Continuous Aligned Polyvinylpyrrolidone Fibers via Electrospinning by Elimination of the Jet Bending Instability. *J. Appl. Poly. Sci.* **116**, 3676–3681 (2010)

30. Ji, C. et al. Suspended, Straightened Carbon Nanotube Arrays by Gel Chapping. *ACS Nano* **5**, 5656–5661 (2011).

31. Srivastava, S. et al. Light-Controlled Self-Assembly of Semiconductor Nanoparticles into Twisted Ribbons. *Science* **327**, 1355–1359 (2010).

32. Gates, B. D., Xu, Q. B., Stewart, M., Ryan, D., Willson, C. G. & Whitesides, G. M. New approaches to nanofabrication: Molding, printing, and other techniques. *Chem. Rev.* **105**, 1171–1196 (2005).

33. Liu, J. W., Xu, J., Ni, Y., Fan, F. J., Zhang, C. L. & Yu, S. H. A Family of Carbon Based Nanocomposite Tubular Structures Created by In Situ Electron Beam Irradiation. *ACS Nano* **6**, 4500–4507 (2012) .

34. Banholzer, M. J., Millstone, J. E., Qin, L. & Mirkin, C. A. Rationally designed nanostructures for surface-enhanced Raman spectroscopy. *Chem. Soc. Rev.* **37**, 885–897 (2008).

35. Fleischmann, M., Hendra, P. J. & McQuillan, A. J. Raman spectra of pyridine adsorbed at a silver electrode. *Chem. Phys. Lett.* **26**, 163–166 (1974).

36. Lu, G., Li, H., Liusman, C., Yin, Z. Y., Wu, S. X. & Zhang, H. Surface enhanced Raman scattering of Ag or Au nanoparticle-decorated reduced graphene oxide for detection of aromatic molecules. *Chem. Sci.* **2**, 1817–1821 (2011).

37. Tao, A. R. & Yang, P. D. Polarized surface-enhanced Raman spectroscopy on coupled metallic nanowires. *J. Phys. Chem. B* **109**, 15687–15690 (2005).

38. Gunawidjaja, R., Peleshanko, S., Ko, H. & Tsukruk, V. V. Bimetallic nanocobs: Decorating silver nanowires with gold nanoparticles. *Adv. Mater.* **20**, 1544–1549 (2008).

39. Chang, S., Ko, H., Gunawidjaja, R. & Tsukruk, V. V. Raman Markers from Silver Nanowire Crossbars. *J. Phys. Chem. C* **115**, 4387–4394 (2011).

40. Yang, C. et al. Silver Nanowires: From Scalable Synthesis to Recyclable Foldable Electronics. *Adv. Mater.* **23**, 3052–3056 (2011).

41. Qian, H. S., Yu, S. H., Gong, J. Y., Luo, L. B. & Fei, L. F. High-quality luminescent tellurium nanowires of several nanometers in diameter and high aspect ratio synthesized by a poly (vinyl pyrrolidone)-assisted hydrothermal process. *Langmuir* **22**, 3830–3835 (2006).

42. Zhang, G., Yu, Q., Yao, Z. & Li, X. Large scale highly crystalline Bi_2Te_3 nanotubes through solution phase nanoscale Kirkendall effect fabrication. *Chem. Comm.* **17**, 2317–2319 (2009).

43. Liu, H. & Lalanne, P. Microscopic theory of the extraordinary optical transmission. *Nature* **452**, 728–731 (2008).

44. Gordon, R., Sinton, D., Kavanagh, K. L. & Brolo, A. G. A New Generation of Sensors Based on Extraordinary Optical Transmission. *Acc. Chem.Res.* **41**, 1049–1057 (2008).

45. Wang, H. H. et al. Highly Raman-Enhancing Substrates Based on Silver Nanoparticle Arrays with Tunable Sub-10 nm Gaps. *Adv. Mater.* **18**, 491–495 (2006).

46. Lee, S. J., Morrill, A. R. & Moskovits, M. Hot Spots in Silver Nanowire Bundles for Surface-Enhanced Raman Spectroscopy. *J. Am. Chem. Soc.* **128**, 2200–2201 (2006).

47. Jiang, Bosnick, K., Maillard, M. & Brus, L. Single Molecule Raman Spectroscopy at the Junctions of Large Ag Nanocrystals. *J. Phys. Chem. B* **107**, 9964–9972 (2003).

48. Mohanty, P. et al. Simple Vapor-Phase Synthesis of Single-Crystalline Ag Nanowires and Single-Nanowire Surface-Enhanced Raman Scattering. *J. Am. Chem. Soc.* **129**, 9576–9577 (2007).

49. Song, C., Abell, J. L., He, Y., Hunyadi Murph, S., Cui, Y. & Zhao, Y. Gold-modified silver nanorod arrays: growth dynamics and improved SERS properties. *J. Mater. Chem.* **22**, 1150–1159 (2012).

50. Singh, J. P., Lanier, T. E., Zhu, H., Dennis, W. M., Tripp, R. A. & Zhao, Y. Highly Sensitive and Transparent Surface Enhanced Raman Scattering Substrates Made by Active Coldly Condensed Ag Nanorod Arrays. *J. Phys. Chem. C* **116**, 20550–20557 (2012).

51. Sun, Y. & Wiederrecht, G. P. Surfactantless Synthesis of Silver Nanoplates and Their Application in SERS. *Small* **3**, 1964–1975 (2007).

52. Hsiao, W.-H., Chen, H.-Y., Yang, Y.-C., Chen, Y.-L., Lee, C.-Y. & Chiu, H.-T. Surface-Enhanced Raman Scattering Imaging of a Single Molecule on Urchin-like Silver Nanowires. *ACS Appl. Mater. & Interfaces* **3**, 3280–3284 (2011).

53. Tao, A. et al. Langmuir−Blodgett Silver Nanowire Monolayers for Molecular Sensing Using Surface-Enhanced Raman Spectroscopy. *Nano Lett* **3**, 1229–1233 (2003).

Acknowledgements

Author contributions

J.W.L. planned and performed the experiments, collected and analysed the data, and wrote the paper. S.H.Y. supervised the project, conceived the experiments, analysed the results and wrote the paper. J.L.W., W.R.H. and W.C.W. helped with synthesis of the materials and collected the data. L.Y. and X.F.R. were responsible for transmission spectra analysis.

Additional information

How to cite this article: Liu, J. *et al.* Ordering Ag nanowire arrays by a glass capillary: A portable, reusable and durable SERS substrate. *Sci. Rep.* **2**, 987; DOI:10.1038/srep00987 (2012).